Journal of Materials Chemistry B

Accepted Manuscript

ROYAL SOCIETY OF CHEMISTRY

www.rsc.org/materialsB

Journal Name Journal of Materials Chemistry B Dynamic Article Links ▶

Cite this: DOI: 10.1039/c0xx00000x

www.rsc.org/xxxxxx

ARTICLE TYPE

Size effects of self-assembled block copolymers spherical micelles and vesicle on cellular uptake in human colon carcinoma cells

Teddy Chang[1], Megan S. Lord[3,*] Björn Bergmann,[1,2] Alex Macmillan[4] and Martina H. Stenzel[1,*]

Received (in XXX, XXX) Xth XXXXXXXXX 20XX, Accepted Xth XXXXXXXXX 20XX
DOI: 10.1039/b000000x

Block copolymers, poly(oligo ethylene glycol methyl ether methacrylate)-*block*-poly(styrene), POEGMEMA-b-PS, with various block length were prepared via RAFT polymerization and subsequently self-assembled into various aggregates to investigate their uptake ability into human colon carcinoma cell line, WiDr. By varying the ratio of the hydrophobic to hydrophilic block length in the block copolymers various morphologies including spherical micelles, cylindrical micelles (rods), vesicles and large compound micelles could be generated. With increasing length of the hydrophobic block the micelles grew in size until chain stretching caused the transition to rods then other aggregates. Micelles of two sizes with a hydrodynamic diameter of 34 and 49 nm, respectively and two different vesicles (hydrodynamic diameter 99 nm and 150 nm) were further studied towards their ability to be taken up human colon carcinoma cells. Results indicated that the smaller sized micelles were taken up almost immediately while an increased sized micelle were taken up, however at a slower rate. Though larger vesicle aggregates were taken up at a slower rate, but eventually all cells internalized aggregates to a similar amount after a few hours.

.

Introduction

Cellular uptake of nanoparticles is often considered pivotal to deliver of drugs to the intracellular target.[1, 2] In studying the cellular uptake ability of nanoparticles with the absence of any cell-penetrating peptides, the amount of nanoparticles found intracellular is dependent on surface chemistry, size and shape.[3-5] Nanoparticles of 50 nm are often highlighted as optimum size to achieve maximum cell uptake,[6, 7] while increasing aspect ratio in rod-like structures delay the uptake.[6] Most studies have been carried out using inorganic nanoparticles, foremost gold nanoparticles.

Polymer-based nanoparticles have been widely explored for their ability to encapsulate a broad variety of drugs while their size can be tailored with ease by polymerization and processing conditions. While a strong focus on spherical polymer particles in the literature is apparent, vesicles have a similar spherical shape however have a hollow aqueous core different than the hydrophobic polymeric core of the traditional micelles.[8] A convenient way to generate vesicle structures is by the means of self-assembled block copolymers. Amphiphilic block copolymer are able to self-assembly in selective solvents into a wide variety of structures ranging from spherical micelles to cylindrical micelles (rods), vesicles, bilayers and a range of non-equilibrium structures.[9-11] Polymeric micelles, including block co-polymer micelles, have been extensively investigated for drug delivery applications.[12, 13] These structures enable drugs to be encapsulated in the hydrophobic core while the hydrophilic shell can protect the incorporated drug while altering pharmacokinetic and biodistribution properties favorably.[14, 15] Polymeric micelles offer great flexibility in the block copolymer chemistry allowing the modification and functionalization of the core and shell of the nanostructure for targeted delivery purposes. Depending on the polymer composition and the preparation conditions, amphiphilic block copolymers can also form vesicular assemblies. These reflect the structure of liposomes in the way that a bilayer structure is present which encloses an aqueous interior and are considered to be more rigid, stable and versatile[16]

Various other self-assembled polymeric structures, such as "crew-cut" aggregates,[17] can be produced by changing the lengths of both the hydrophilic and hydrophobic blocks. A short hydrophobic block compared to the hydrophilic block leads to the formation of spherical micelles, while extending the length of the hydrophobic block may result in an increase in size of the micelles, as well as the transition in the morphology to vesicles, due to stretching of polymer chains within the core. The final morphology is dependent on the copolymer composition, preparation method and also copolymer polydispersity [18-20]. The morphological transition behaviour from spheres to rods has been investigated in detail on series of poly(acrylic acid)-poly(styrene), PAA-PS [21] and poly(ethylene)-poly(styrene), PEO-PS [22, 23] copolymers while these polymers have also been shown to

produce lamellae, tubules, vesicles, large compound micelles (LCMs) and large compound vesicles (LCVs) morphologies.[24] A "flowerlike" morphology has also been reported with self-assembled amphiphilic thermo-responsive ABA triblock copolymer with methyl methacrylate (MMA) (A blocks), and N-isopropylacrylamide (NIPAMM) (copolymerized with polyethylene glycol methyl ether methacrylate (PEGMEMA) for the B block).[25]

The cellular uptake of micelles has been moderately studied in literature using mainly micelles based on poly(ethylene oxide) (PEO)-based block copolymers.[26, 27] The uptake is determined by parameters such as size and surface chemistry similar to rigid nanomaterials.[28] Polymeric nanoparticles have been widely reported to be rapidly internalized by cells within 1 – 15 min *in vitro* reaching a maximum internalization level with 24 h of exposure in a variety of cell lines.[29, 30] However, the dynamic character of micelles adds a new level of complication. At low concentrations, well below the critical micelle concentration (CMC), the micelles disassociate and while the uptake of the polymer cannot be observed anymore in some cases,[31] the triblock copolymer PEO-PPO-PEO in its unimer state seems to interact favourably with the cell membrane.

Only a few reports dealt with the uptake of other aggregates than spherical micelles although vesicles while larger in size offer advantages in the use of a drug delivery vehicle with their hollow aqueous core.[8] Vesicles can be used as carriers of hydrophobic drugs (in the bilayer) as well as hydrophilic drugs (in the interior) making them an attractive structure for purposes of drug delivery. Therefore, the aim of this study was to synthesize block copolymers based on oligoethylene glycol methyl ether methacrylate (OEGMEMA) and polystyrene (PS) via RAFT polymerization[32, 33] to create a variety of morphologies. POEGMEMA has been chosen as an alternative for PEO since a range of recently developed drug delivery carriers are based on this polymer and therefore this type of polymer warrants investigation.[34-36] Focus of this study was to investigate the amount and rate of uptake into human colon carcinoma cell line, WiDr. Morphology of the polymers was varied by adjusting the ratio of the block copolymers with a fixed hydrophilic POEGMEMA block length. Using PEGMEMA even with the bulk side group resulted in the use of a larger block of PS. This large hydrophobic group caused the core stretching that resulted in the larger morphologies including the vesicles.

MATERIALS AND METHODS

Materials

Styrene (99% pure, Aldrich) was passed through a column of basic alumina to remove inhibitor immediately prior to use. 2,2-Azobis(isobutyronitrile) (AIBN, 98% pure, Fluka) was recrystallized twice from methanol prior to use. 1,3-Diissopropenylbenzene (Aldrich, 97%), tetrahydrofuran (THF, HPLC grade, LAB-SCAN, 99.8%), toluene (HPLC grade, LAB-SCAN, 99.8 %), *n*-hexane (AR grade, UNIVAR), anhydrous methanol (MeOH, 99.9 % pure, Mallinckrodt), chloroform (99% pure, LAB- SCAN), dimethylformamide (DMF, 99 % Aldrich), were obtained at the highest purity and used without further purification unless otherwise stated. LysoTracker Red DND-99 was purchased from Life Technologies. All well plates used were purchased from Greiner Bio One.

Synthesis of Polymers

Synthesis of POEGMEMA MacroRAFT agent

The macroRAFT was prepared with monomer oligo ethylene glycol methyl ether methacrylate (M_n = 300 g/mol) (7.257 mL, 7.620 g, 25.4 mmol) which was passed through a column of basic alumina to remove inhibitor prior to polymerization, RAFT agent cyanopentanoic acid dithiobenzoate (CPADB) (0.0710 g, 0.2541 mmol), o-fluorescein methacrylate (0.0051 g, 0.0254 mmol) and initiator AIBN (0.00834 g, 0.05079 mmol) at ratio of (Monomer: Fluorescein: RAFT = 100:1:1; Monomer: AIBN = 500:1). The mixture was placed in a round bottom flask and dissolved in 40 mL of toluene. The reaction mixture was placed in an ice bath and purged with nitrogen for 30 min. The reaction mixtures were then immersed in an oil bath at 70˚C and samples were taken over a period of 24 h. The polymerization was terminated by placing the samples in an ice bath for 5 min.

^{1}H NMR was used to determine the conversion of the monomers by comparing the intensity of vinyl proton peaks (6.1 and 5.6 ppm) to that of aliphatic proton peaks (1.1–1.3 ppm). The polymers were purified three times by precipitation in petroleum spirits (B_p of 40–60˚C) followed by centrifugation at 7000 rpm for 15 min and drying in a vacuum at 30˚C. Purification was confirmed through ^{1}H NMR through the absence of monomer peaks.

Synthesis of POEGMEMA-block-Polystyrene

To synthesize the di-block copolymer the macroRAFT with a small M_n (~4000 g/mol) and low number of repeating units (~15) was chosen for chain extension with styrene (Scheme 1). The ratio of POEGMEMA marcoRAFT agent to styrene was adjusted from 1:300 to as high as 1:3000. The reaction was carried out according to Table 1 while continually changing the molar ratio of styrene. The macroRAFT agent (0.1 g, 2.6×10^{-5} mol) and AIBN (0.00026 g, 1.6×10^{-6} mmol) were dissolved styrene (0.81 g, 7.8×10^{-3} mmol) leading to a ratio of ([Monomer]:[RAFT]:[AIBN] = 300:1:0.1). The reaction mixture was then purged with nitrogen for 1 h in an ice bath. The polymerizations were carried out in an oil bath at 100˚C. The vials were taken out at different time intervals over a period of 72 h. The polymerizations were terminated by placing the samples in an ice bath for 5 min. The copolymers were purified by placing the solution into a weighing dish and allowing the volatile styrene monomer to evaporate in the fumehood for 24 h. Conversion was calculated through the following equation:

$$\text{Conversion} = \frac{W_P - W_D}{W_S - W_D} \times 100$$

where, W_D is the weight of the empty dish, W_P is the weight of the dish after 24 h evaporation, W_S is the weight of dish with polymer solution. The purity of the resulting copolymer after evaporation was confirmed through ^{1}H NMR showing no monomer peaks were present.

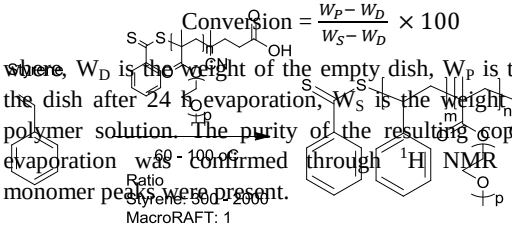

Scheme 1. Synthesis of POEGMEMA-b-PS.

Self-Assembly POEGMEMA-block-PolyStyrene

10 mg of the block copolymer was dissolved in 1 mL of DMF. The solution was then placed on a stir plate with a high rate of

stirring at room temperature. Deionized water was added dropwise to the solution until a concentration of 2 mg/mL was obtained. The solution was then place into a dialysis membrane with pore size M_W < 3500 and dialyzed against deionized water for 24 h.

Characterization of polymers and micelles

Gel Permeation Chromatography (GPC). The molecular weight and polydispersity of prepared polymers was obtained via size exclusion chromatography (SEC). The eluent was N,N-dimethylacetamide (DMAc) [DMAc; 0.03% w/v LiBr, 0.05% w/v 2,6-di-butyl-4-methylphenol (BHT)] at 50 °C (flow rate of 1 mL/min) with a Shimadzu modular system comprising a SIL-10AD auto-injector, a Polymer Laboratories 5.0-lm bead-size guard column (50 x 7.8 mm) followed by four linear PL (Styragel) columns (105, 104, 103, and 500 Å) and an RID-10A differential refractive-index detector. The SEC calibration was performed with narrow-polydispersity polystyrene standards ranging from 168 to 106 g mol^{-1}. 50 mL of polymer solution (2 mg/mL in DMAc) was injected for every analysis.

Nuclear Magnetic Resonance (NMR) spectroscopy. All NMR spectra were recorded using a Bruker 300 MHz spectrometer. All chemical shifts are reported in ppm (d) relative to tetramethylsilane, referenced to the chemical shifts of residual solvent resonances (^{1}H and ^{13}C). The following abbreviations were used to explain the multiplicities: s for singlet, d for doublet, t for triplet, m for multiplet and bs for broad singlet.

Dynamic Light Scattering (DLS). The average diameters and size distributions of the micelles prepared in either deionized water or cell culture medium were measured using a Malvern Zetaplus particle size analyzer (laser, 35 mW, λ = 632 nm; angle 90°) at a polymer concentration of 2 mg/mL. Samples were filtered to remove dust using a microfilter 0.45 µm prior to the measurements.

Transmission Electron Microscopy (TEM). TEM micrographs were obtained using a JEOL 1400 transmission electron microscope. The samples were prepared by casting the micellar solution (1 mg/mL) onto a formvar-coated copper grid. The samples for TEM were positively stained with 2 % osmium tetroxide vapor.

Scanning Electron Microscope (SEM). SEM images were collected on a NanoSEM 230 microscope. The samples were prepared at concentration 2 mg/mL on copper tape. The samples were dropped on the copper tape and were allowed to settle for 1 min prior to using filter paper to remove the water. The samples were then coated with chromium using an Emitech K575x Chromium Sputter Coater.

Culture of human colon carcinoma cell line, WiDr

The human colon carcinoma cell line, WiDr, was maintained in Dulbecco's modified eagle medium (DMEM) supplemented with 2.2 g/L $NaHCO_3$, 10 % (v/v) foetal bovine serum (FBS), 100 U/mL penicillin and 100 µg/mL streptomycin in a humidified incubator (5 % CO_2 / 95 % air atmosphere at 37 °C).

Cell viability analysis

WiDr cells were seeded in 24-well tissue culture polystyrene plates at a density of 1×10^4 cells/well in 1 mL culture medium at polymer aggregates were added at a final concentration of 500 µg/mL. Cell viability was analysed at 24 and 48 h after the addition of polymer aggregates using an automated cell viability analyzer (ViCell, Beckman Coulter, Sydney, Australia) that is based on trypan blue exclusion dye analysis.

Cellular Uptake

Flow Cytometry (FC). Polymer uptake was measured by flow cytometry by measuring fluorescence intensity. WiDr cells were seeded in 6-well tissue culture polystyrene plates at a density of 5×10^5 cells/well in 3 mL culture medium and 50, 100 and 500 µg/mL polymer aggregates. Cells were analyzed after 1, 2, 4 and 24 h. For each sample, data was acquired for 1×10^4 gated events using a flow cytometer (BD FACSort) by measuring fluorescence intensity along with the number of cells. Data were analysed using the FCS 4 Express software.

Confocal Fluorescence Microscopy. WiDr cells were seeded into 35 mm diameter (9.6 cm^2) dishes at a density of 5×10^5 cells/well in 3 mL of culture medium and allowed to attach to the dish for 16 h before experimentation. Cells were stained with Lysotracker red (1:20 000 in culture medium) for 30 min at 37ºC. Cells were then rinsed with DPBS and exposed to fresh culture medium for imaging. Cells were exposed to various concentration of polymer aggregates and live cell imaging was initiated immediately following exposure to the polymers using a Leica TCS SP5 confocal fluorescence microscope over a period of 24 h.

Statistical Analysis

A t test (two samples, two tailed distribution assuming equal variance) was used to compare statistical significance. $p < 0.05$ results were considered significant. Experiments were performed in triplicate and experiments were repeated.

RESULTS AND DISCUSSION

Polymer synthesis and self-assembly

The RAFT agent was used in the polymerization with POEGMEMA in toluene at 70˚C and the conversion of the monomer was determined through ^{1}H NMR (Figure S1, ESI) with the results summarized in Table S1, ESI. The monomer conversion increased with reaction time while the radical concentration was constant during the course of polymerization as demonstrated by a pseudo first order plot (Figure S2 A, ESI). The theoretical and experimental molecular weights were proportional to the monomer conversion (Table S2). The experimental molecular weight increased linearly with the monomer conversions and the polydispersity index (PDI) remained low (<1.20). The low PDI over the course of the reaction is an integral property that indicates a well-controlled RAFT polymerization. The purified polymers were subsequently employed in the self-assembly process without further removal of the RAFT endgroup, which can be easily cleaved using a range of conditions.[37, 38]

Preliminary studies in our lab showed that long POEGMEMA blocks mainly led to aggregates such as micelles even if the PS block was substantially longer. To generate crew-cut aggregates such as vesicles, the smallest POEGMEMA macroRAFT agent with a molecular weight of M_n(theo)=3900 g mol^{-1} was chosen for chain extension with styrene. The POEGMEMA macroRAFT

agent was then polymerized with styrene at a ratio significantly larger than the hydrophilic POEGMEMA block. The ratio between hydrophilic monomer and hydrophobic monomer concentration was varied in the range of 300 to 3000 in order to obtain micelle structures as well as various crew-cut aggregates. Although the RAFT agent chosen was expected to undergo an efficient chain transfer process,[13] low RAFT agent concentrations, such as 3000:1 monomer to RAFT agent ratio, may exceed the limits of the RAFT process.

The polymerization of styrene was carried out in bulk and after different time intervals the monomer conversion was determined using ^{1}H-NMR (ESI, Figure S3). Consumption of the monomer was retarded with increasing macroRAFT agent concentration, which is in good agreement with the expected behavior.[39] The molecular weight was found to increase with increasing conversion (Table S2 and Figure S4). However, at high monomer to RAFT agent ratios the molecular weight distribution of polymer started to broaden, which is particularly pronounced at higher conversions, and significantly deviated from the theoretical molecular weight. This is likely due to the relatively low concentration of the RAFT agent, which led to insufficient suppression of the termination reaction leading to increasing amounts of non-RAFT polymer, possibility PS. Block copolymers with numbers of repeating units up to 1000 all had a PDI of 1.4 or less. Block copolymers with longer PS blocks typically have PDI > 1.4 which is indicative of a process that is less well-controlled and likely to contain some terminated polymer as impurity.

The block copolymers were purified and dissolved in DMF, followed by the very slow addition of water and the subsequent dialysis. The aggregates were analyzed by DLS, which showed that the hydrodynamic diameter increased as the size of the hydrophobic chain increased (Figure 1). It was expected that a small hydrophobic PS block compared to the hydrophilic POEGMEMA block would lead to spherical micelles. With the increasing length of the hydrophobic block the size of the micelle was expected to grow until the necessary chain stretching of the PS block became entropically unfavorable leading to the transition of cylindrical micelles (rods) and vesicles (polymersomes).[18] A large catalogue of other structures can also be created, which are often in co-existence with each other. TEM and SEM were used to confirm the formation of micelles at low hydrophobic block lengths and crew-cut aggregates at longer hydrophobic block lengths (Figure 2). The low block length of the hydrophilic POEGMEMA in combination with the low block length of the hydrophobic styrene (typically below 500 styrene RUs) resulted in spherical micelles (Figure 2 A - D). The diameters of these micelles measured by TEM and SEM were in agreement with the DLS measurements with particle diameters in the range of 30 – 70 nm. Some micelles were found to have a wide particle size range, such as in Figure 2D. The majority of these micelles had a diameter less than 100 nm as measured by SEM however the larger particles affected the volume-average hydrodynamic diameter measured using DLS which was found to be 150 nm (Figure 1). The transition from micelles to rods took place at styrene RU greater than 200 (Figure 2, E). DLS is modeled on the diffusion of a sphere and indicated that the diameter of these rods were 150 - 250 nm, however TEM and SEM indicated that the diameter of these rods was below 100 nm while the length exceeded 1 µm. Some of the rods exhibited a pearl-necklace appearance, which are indicative of the two-step transition of spheres to rods [40, 41]. The next morphological transition took place when POEGMEMA had only a very small number of repeating units (N=13) and the PS block was higher than 500 (Figure 2 F). Large compound micelles (LCM) formed at styrene RU greater than 2300 (Figure 1, H-I) which is in agreement with a previous report [42]. The vesicles and LCMs were more spherical in nature which resulted in good agreement between TEM, SEM and DLS for the average particle size which was between 150 to 250 nm (Figure 1). Some TEMs showed the co-existence of two morphologies next to each other and the circles in Figure 1 that should indicate the obtained morphology should only act as guidance.

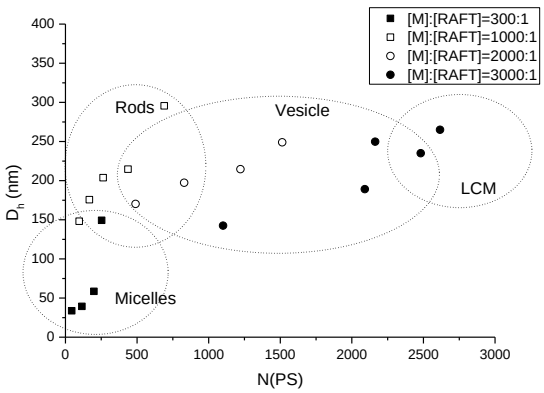

Fig.1 The hydrodynamic diameter, D_h (nm) vs. N_{PS} of aggregates determined using DLS (c= 2 mg mL^{-1} in deionized water). (A) [POEGMEMA macroRAFT] : [Styrene] = 1 : 300, (B) [POEGMEMA macroRAFT] : [Styrene] = 1 : 1000, (C) [POEGMEMA macroRAFT] : [Styrene] = 1 : 2000, (D) [POEGMEMA macroRAFT] : [Styrene] = 1 : 3000.

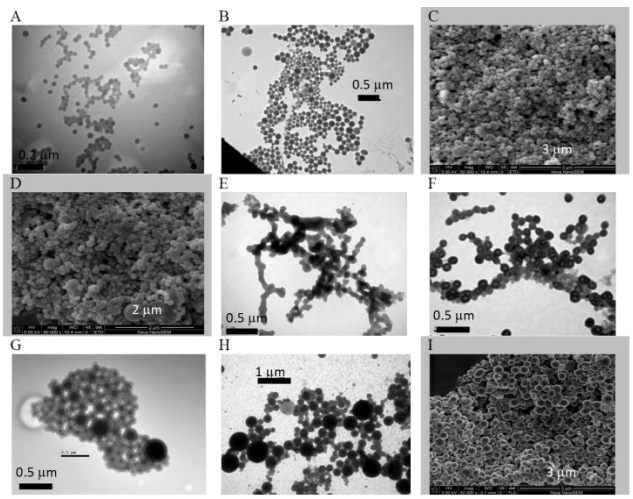

Fig.2 : TEM or SEM (grey background) analysis of the aggregates (concentration of polymer 2mg mL^{-1} in water) of (A) PEGMEMA $_{13}$-PSTY$_{54}$, (B) PEGMEMA $_{13}$-PSTY$_{89}$, (C) PEGMEMA $_{13}$-PSTY$_{114}$, (D) PEGMEMA $_{13}$-PSTY$_{189}$, (E) PEGMEMA $_{13}$-PSTY$_{250}$, (F) PEGMEMA $_{13}$-PSTY$_{2008}$, (G) PEGMEMA $_{13}$-PSTY$_{2265}$, (H) PEGMEMA $_{13}$-PSTY$_{2631}$, (I) PEGMEMA $_{13}$-PSTY$_{2876}$

A large array of block copolymers were subsequently prepared using a variety of POEGMEMA macroRAFT agents (Figure 3). Micelles were formed over a range of POEGMEMA block lengths at low styrene block lengths. Rod-like structures were obtained when the POEGMEMA block was above 20 repeating units, while the PS block needed to be sufficiently large. Very short POEGMEMA blocks led either to vesicles or LCMs, which is in good agreement with the literature.[18] LCMs are created from the aggregation of inverse micelles that are coated with block copolymers with POEGMEMA that created the water-soluble shell [42].

It seems therefore that very long PS blocks are required to force the transition of micelles to other aggregates. This can be understood considering the large volume of the POEGMEMA polymer.

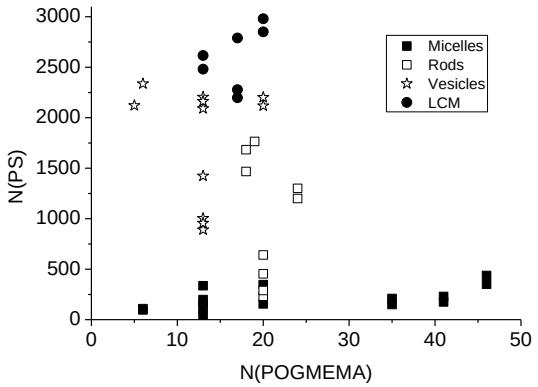

Fig.3 Morphologies of block copolymers as a function of their respective block lengths of hydrophilic POEGMEMA and hydrophobic styrene.

Employing the same synthesis technique as the polymer aggregates formed in Figure 1 and 2 a new set of polymers were formed with a fluorescent tag chemically linked to them. These block copolymers were subsequently employed to investigate their interaction with cells (Table 1). In order to investigate the cellular uptake properties of the various aggregates a fluorescent monomer was incorporated into the POEGMEMA macroRAFT agent at 1 mol %. The fluorescence intensity of each of the polymers was found to be related of the size of the block copolymer with the smaller block copolymers having a greater intensity than the larger polymers (Figure S5).

The polymer aggregates were formed, analyzed and stored in deionized water. To ensure that they would maintain the same morphologies when exposed to cell culture medium, DLS was also performed in cell culture medium. The size of the polymer aggregates was the same in deionized water and cell culture medium (Table 1). The polymer aggregates tested are seen in the TEM (Figure 3) and will be referred to herein by their aggregate type and diameter in DI water. A variation of diameter and dispersity of size from the TEM images compared to DLS data is derived due to the dry state conditions of the TEM samples compared to the aqueous condition of the DLS.

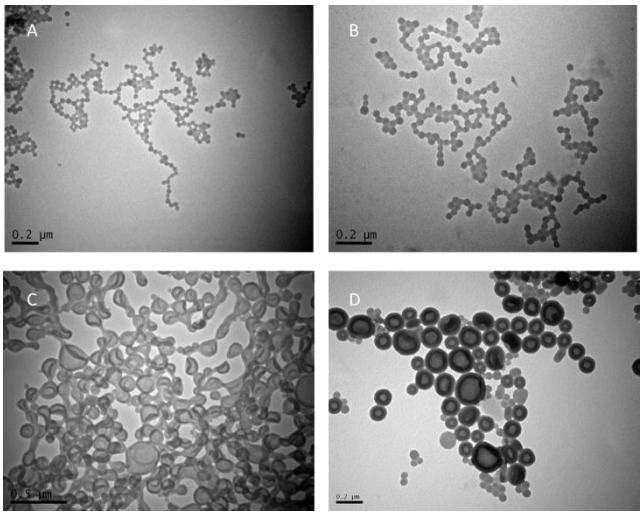

Fig.4 TEM analysis of the aggregates (concentration of polymer 2 mg mL^{-1} in water) of (A) 34 nm micelles, (B) 49 nm micelles, (C) 99 nm vesicles and (D) 150 nm vesicles

Table 1 The polymer aggregates size measured by DLS in DI water and cell culture medium, DMEM. The number of RUs is stated with each block as well the aggregate formed.

		Diameter (nm)	
Polymer	**Aggregate type**	**DI Water**	**DMEM**
$POEGMEMA_{12}$-PS_{44}	Micelle	34 ± 4	32 ± 3
$POEGMEMA_{12}$-PS_{53}	Micelle	49 ± 5	51 ± 6
$POEGMEMA_{12}$-PS_{595}	Vesicle	99 ± 11	90 ± 10
$POEGMEMA_{12}$-PS_{648}	Vesicle	150 ± 17	144 ± 17

The stability of the aggregates can also be expressed by their critical micelle concentration (CMC). Polymeric micelles can disassemble into unimers at low concentrations below their CMC or when changes in temperature, pH, or ionic strength occur. The CMC of $POEGMA_{40}$-*b*-PS_{99} in aqueous solution was measured to be 14 mg/L with the surface tension at the CMC of 56 mN/m.[43] In addition, the break-up of micelles is kinetically hampered and the micelle are known to be stable well below their CMC [44] although recent studies have shown that micelles, especially with smaller hydrophobic blocks, can break up during *in vitro* studies [45-47]. The concentration of the aggregates used in these experiments were at much higher concentrations than these block copolymers and well above the CMCs indicating that the aggregates will be stable in the cell culture medium.

Cell interactions with POEGMEMA-PS micelles and vesicles

The proliferation of WiDr cells in contact with the polymers was investigated at a concentration of 500 µg/mL over a period of 48 h (Figure 4). None of the polymeric micelles were found to significantly reduce cell proliferation over the 48 h analysis period ($p < 0.05$) compared to cells exposed to normal growth conditions.

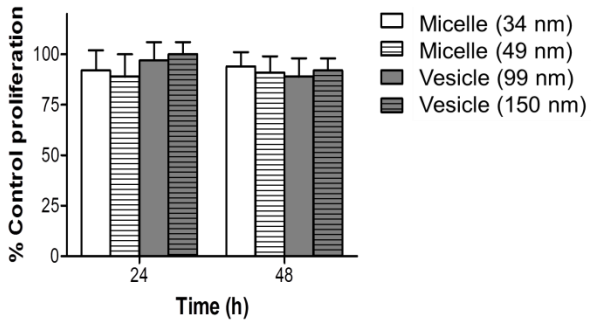

Fig.5 Cell viability of WiDr cells exposed to 500 µg/mL polymer aggregates compared to cells exposed to medium only (control proliferation) analysed over a period of 48 h. Data presented as mean ± standard deviation (n = 3).

Uptake of the polymer aggregates into the WiDr cells was measured using two techniques, flow cytometry and fluorescence spectroscopy. The first method analyses the number of cells that have fluorescing material internalized, while the latter technique quantified the fluorescence of the cell growth media, which results in the amount of aggregates that have not been taken up. Both techniques are complementary, but offer quantitative results from a different perspective.

Uptake of the polymer aggregates into the WiDr cells was analyzed after 24 h of exposure to the different sized micelles at a concentration of either 50 or 500 µg/mL by flow cytometry by measuring fluorescence intensity (Figure 6). The fluorescent monomer was chemically linked to the polymers, so increased fluorescence intensity indicated polymer uptake into cells, however each polymer was found to have a different level of fluorescence (Figure S5). Hence, comparison of the uptake of each polymer aggregate can be made, but not directly between polymers. Cells were found to internalize each of the polymer aggregates in a dose-dependent fashion as shown by the increased fluorescence intensity profiles for cells exposed to the highest concentration of each of the polymer aggregates compared to the lowest concentration tested and cells exposed to medium only (Figure 6). All cells exposed to the 34 nm micelles and the 99 nm vesicles at both concentrations were found to internalize the polymer aggregates (Figure 6 A and C) while not all cells internalized the larger micelles and vesicle (Figure 6 B and D). Only 55% of cells showed internalization to the 49 nm micelles at a concentration of 50 µg/mL after 24 h, while at the higher concentration all cells internalized the micelles (Figure 5 B). Similarly, only 15% of cells showed internalization to the 150 nm vesicles at a concentration of 50 µg/mL after 24 h, while at the higher concentration all cells exhibited internalization to these vesicles (Figure 6 D).

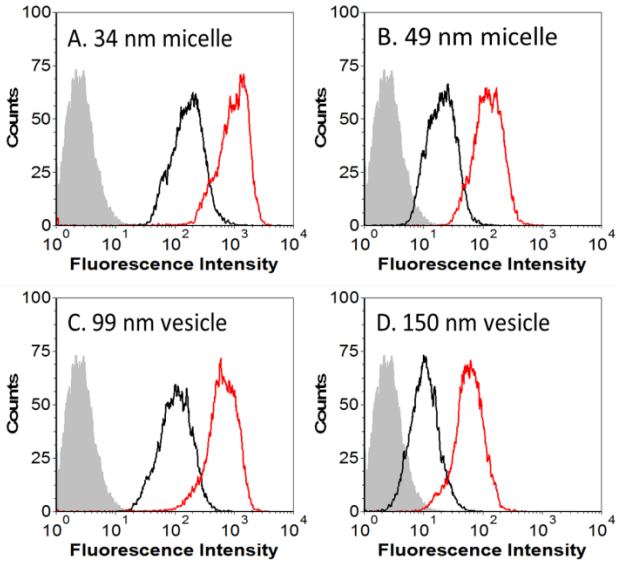

Fig.6 Flow cytometric analysis of polymer aggregate uptake into WiDr cells at 24 h. Cells were exposed to polymer aggregates at a concentration of either 50 or 500 µg/mL including (A) 34 nm micelles, (B) 49 nm micelles, (C) 99 nm vesicles and (D) 150 nm vesicles or medium only control (grey). Uptake was measured by fluorescence intensity of the internalized polymer aggregates at concentrations of 50 (black) or 500 (red) µg/mL.

The uptake was monitored over a period of 24 h at a concentration of 500 µg/mL by flow cytometry by measuring fluorescence intensity. Cells were found to internalize each of the different polymer aggregates within 1 h of exposure (Figure 7). Internalization of the 34 nm micelles increased over the first 2 h of the measurement period and decreased at 4 and 24 h (Figure 7 A). All cells showed internalization to the 49 nm micelles after 1 h and for the 24 h measurement period (Figure 7 B). There were however, changes in the level of micelle uptake per cell over the 24 h measurement period indicating that exocytosis may have occurred. Interestingly, uptake of the 99 nm vesicles continued to increase throughout the measurement period (Figure 7 C) while uptake of the 150 nm vesicles increased throughout the first 4 h and had decreased by 24 h (Figure 7 D). This data indicated that by 24 h of exposure all cells had internalized nanoparticles and together demonstrated that the size of the micelles affected the extent of micelle internalization.

Analysis of uptake of the 34 nm micelles by the WiDr cells was also performed using confocal fluorescence microscopy immediately after exposure of the cells to the polymer aggregates. Uptake of the 34 nm micelles was found to occur within 2 min of exposure to the cells (Figure 8 A) and remained in the cells for the 2 h analysis period (Figure 8). No change in lysosome expression was observed throughout the experiment. Rapid uptake of polymeric nanoparticles has previously been reported [29, 30] with 97 nm poly(D,L-lactide-coglycolide) nanoparticles taken up by human smooth muscle cells within 2 min [30]. Diblock copolymers based on methoxypolyethylene glycol-block-poly(caprolactone) have also been reported to be internalized by human colon adenocarcinoma cells within 15 min [29].

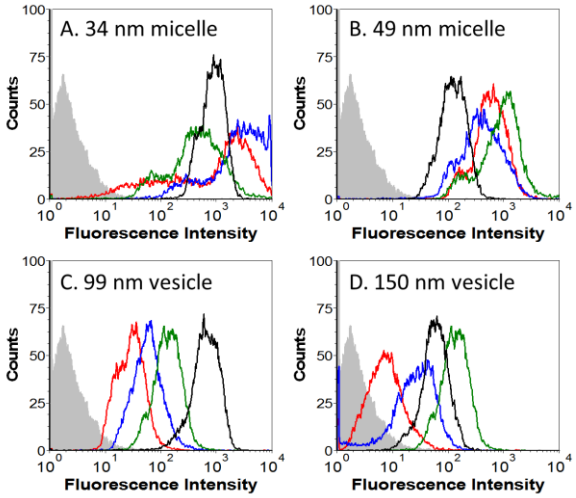

Fig.7 Flow cytometric analysis of polymer aggregate uptake into WiDr cells over a period of 24 h. Cells were exposed to polymer aggregates at a concentration of 500 µg/mL including (A) 34 nm micelles, (B) 49 nm micelles, (C) 99 nm vesicle and (D) 150 nm vesicle or medium only control (grey). Uptake was measured by fluorescence intensity of the internalized polymer aggregates after exposure times of 1 (red), 2 (blue), 4 (green) and 24 (black) h.

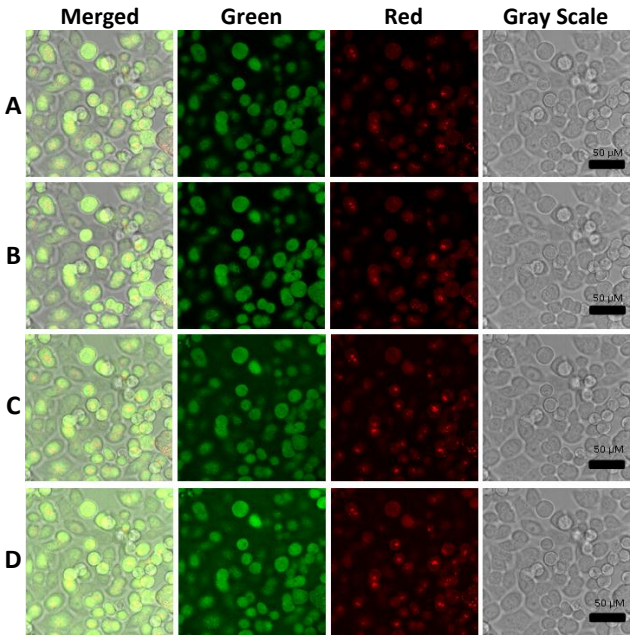

Fig.8 Uptake of 34 nm micelles into WiDr cells after (A) 2, (B) 10, (C) 30 or (D) 120 minutes as measured by confocal fluorescence microscopy when exposed to the polymer aggregates at a concentration of 500 µg/mL. The cell lysosomes were stained with Lysotracker Red (red) while the micelles contain a fluorescein o-methacrylate (green). Scale bar represents 50 µm.

The uptake of other aggregates such as the 150 nm vesicles were monitored over a similar time frame (ESI, Figure S6) showing the increase of fluorescence over a period of 2 hours.

Uptake of the polymer aggregates into cells was also measured by flow cytometry by measuring the forward and side scatters of the cells which indicated cell size and granularity, respectively (Figure 9). Both forward and side scatters were found to increase after 24 h exposure to the different sized nanoparticles. Interestingly, the fluorescence intensity profiles (Figure 6) indicated that all cells internalized the different polymer aggregates, while a large proportion of the cells in each test case did not change either their size or granularity as measured for forward and side scatters (Figure 8). This indicated that a large proportion of the cells took up a low level of polymer aggregates.

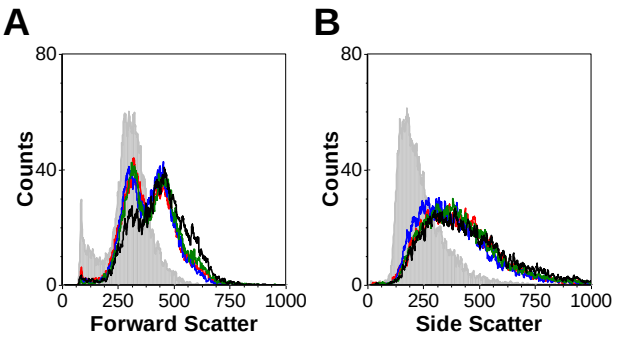

Fig.9 Flow cytometric analysis of (A) forward and (B) side scatter for WiDr cells exposed to 500 µg/mL polymer aggregates after 24 h. Data presented for 34 nm micelles (red), 49 nm micelles (blue), 99 nm vesicle (green) and 150 nm vesicle (black) compared to medium only control (grey).

Quantification of the proportion of cells that showed internalization to the different polymer aggregates over time indicated that at the early time points a greater proportion of the cells showed internalization to the micelles than the vesicles while at the later time points all cells internalised polymers (Figure 10 A). The proportion polymer that was internalised by the cells over a period of 6 h was measured by the level of fluorescence remaining in the cell culture medium (Figure 10 B). These data show that a greater proportion of the micelles were internalized by the cells within 1 h of exposure than either of the vesicles which continued throughout the 6 h measurement period. Together these data demonstrate that micelles were taken up to a greater extent than the vesicles, while the 34 nm micelles were internalized to a larger extent than the 49 nm micelles. Similarly, the 99 nm vesicles were internalized to a greater extent than the 150 nm vesicles. This data agrees with the flow cytometry analyses as more of the smaller micelles need to be internalized to result in the same level of forward and side scatters as for a smaller proportion of the larger micelles.

Conclusions

By keeping the chain length of hydrophilic block to hydrophobic block to a low ratio micelles were produced. The hydrophilic block could be synthesized to a low number of repeating units in the order of ~13-30 by keeping the reaction time between 1.5 and 4 h. The number of repeating units increased in a direct correlation to an increase in reaction time yielding a block length accurate to ± 5 repeating units within an approximately 30 minutes window. The addition of the hydrophobic block through chain extension also provided a polymerization method resulting in a similar block length to reaction time correlation. Block lengths could be achieved to a ± 100 repeating unit target within a 4 hour reaction time. To achieve the various sizes of the spherical micelles the chain length could be either decreased or increased with respect to the desired hydrodynamic diameter. When keeping a low ratio of hydrophobic to hydrophilic block micelles

were observed. It was also observed that by as the ratio of hydrophilic block to hydrophobic block increased the formation of other aggregates were possible. The vesicle shaped aggregates were formed as the hydrophilic block was keep down to ~13 repeating units and increased the hydrophobic block to greater than 500 repeating units. TEM and SEM imaging showed the same structures with the corresponding DLS data showing <10% deviation in hydrodynamic diameter for all aggregates.

Polymer aggregates were found to be non-cytotoxic to human colon carcinoma cells which enabled analyses of polymer aggregate uptake into these cells. Cells were found to rapidly take up the polymer aggregates within minutes of exposure. Variations in concentration and exposure time changed the extent of polymer uptake while the size and shape of the polymer aggregates dominated the extent of uptake. The smaller sized polymer aggregates were taken up to a greater extent and more rapidly than the larger polymer aggregates while the micelles taken up more rapidly, and to a larger extent than the vesicle micelles. Together these data demonstrated that the size and shape of the micelles can be tuned to control the extent and kinetics of polymeric micelle internalization into cells.

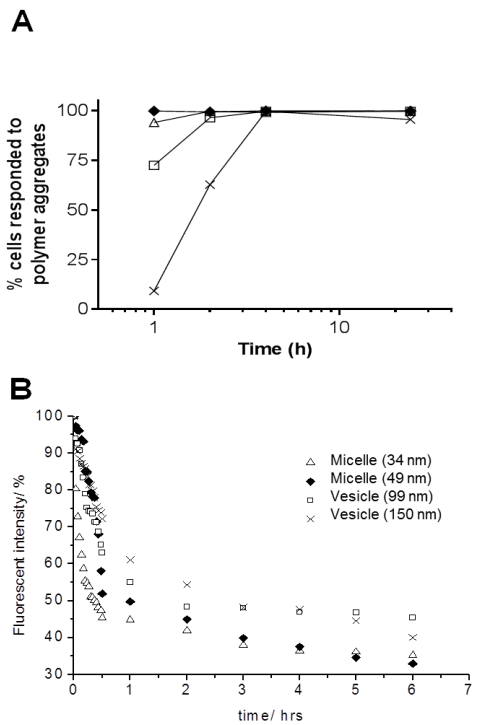

Fig.10 (A) Percentage of cells that showed internalization to the polymer aggregates over 24 h as determined by changes in fluorescence intensity from flow cytometry measurements when WiDr cells were exposed to polymer aggregates at a concentration of 500 µg/mL for a period up to 24 h.(B) Proportion of polymer aggregates remaining in solution after exposure to WiDr cells for a period of 6 h.

Acknowledgements

The authors like to thank the Australian Research Council (FT0991273) for funding. The authors also like to acknowledge the UNSW Mark Wainwright Analytical Centre.

Notes and references

1 Centre for Advanced Macromolecular Design (CAMD), The University of New South Wales, Sydney, NSW 2052, Australia; M.Stenzel@unsw.edu.au
2 Fraunhofer Institute for Chemical Technology ICT, 76327 Karlsruhe, Germany
3 Graduate School of Biomedical Engineering, The University of New South Wales, Sydney, NSW, 2052, Australia; M.Lord@unsw.edu.au
4 Biomedical Imaging Facility, University of New South Wales, Australia 2052

† Electronic Supplementary Information (ESI) available: [NMR of polymers, kinetic data of the polymerization, molecular weights and PDIs of all polymers and fluorescence intensity of the polymers used for the cell work]. See DOI: 10.1039/b000000x/

1. S. R. Abulateefeh, S. G. Spain, K. J. Thurecht, J. W. Aylott, W. C. Chan, M. C. Garnett and C. Alexander, *Biomater. Sci.*, 2013, **1**, 434-442.
2. V. T. Huynh, J. Y. Quek, P. L. de Souza and M. H. Stenzel, *Biomacromolecules*, 2012, **13**, 1010-1023.
3. V. Mailänder and K. Landfester, *Biomacromolecules*, 2009, **10**, 2379-2400.
4. A. Albanese, P. S. Tang and W. C. W. Chan, *Ann. Rev. Biomed. Eng.*, 2012, **14**, 1-16.
5. M. Massignani, C. LoPresti, A. Blanazs, J. Madsen, S. P. Armes, A. L. Lewis and G. Battaglia, *Small*, 2009, **5**, 2424-2432.
6. B. D. Chithrani and W. C. W. Chan, *Nano Letters*, 2007, **7**, 1542-1550.
7. H. Jin, D. A. Heller, R. Sharma and M. S. Strano, *ACS Nano*, 2009, **3**, 149-158.
8. Y. Geng, P. Dalhaimer, S. Cai, R. Tsai, M. Tewari, T. Minko and D. E. Discher, *Nat Nano*, 2007, **2**, 249-255.
9. A. Blanazs, S. P. Armes and A. J. Ryan, *Macromol. Rapid Commun.*, 2009, **30**, 267-277.
10. Y. Y. Mai and A. Eisenberg, *Chem. Soc. Rev.*, 2012, **41**, 5969-5985.
11. D. Quemener, A. Deratani and S. Lecommandoux, in *Constitutional Dynamic Chemistry*, ed. M. Barboiu, Springer-Verlag Berlin, Berlin, 2012, pp. 165-192.
12. K. E. Uhrich, S. M. Cannizzaro, R. S. Langer and K. M. Shakesheff, *Chem. Rev.*, 1999, **99**, 3181-3198.
13. T. Junkers, E. H. H. Wong, Z. Szablan, T. P. Davis, M. H. Stenzel and C. Barner-Kowollik, *Macromol. Rapid Commun.*, 2008, **29**, 503-510.
14. T. Hamaguchi, Y. Matsumura, M. Suzuki, K. Shimizu, R. Goda, I. Nakamura, I. Nakatomi, M. Yokoyama, K. Kataoka and T. Kakizoe, *Br. J. Cancer*, 2005, **92**, 1240-1246.
15. K. Letchford and H. Burt, *Eur. J. Pharm. Biopharm.*, 2007, **65**, 259-269.
16. D. E. Discher and A. Eisenberg, *Science*, 2002, **297**, 967-973.
17. Y. Geng, P. Dalhaimer, S. S. Cai, R. Tsai, M. Tewari, T. Minko and D. E. Discher, *Nature Nanotech.*, 2007, **2**, 249-255.
18. N. S. Cameron, M. K. Corbierre and A. Eisenberg, *Can. J. Chem.*, 1999, **77**, 1311-1326.
19. L. B. Luo and A. Eisenberg, *Langmuir*, 2001, **17**, 6804-6811.
20. L. B. Luo and A. Eisenberg, *J. Am. Chem. Soc.*, 2001, **123**, 1012-1013.
21. L. F. Zhang and A. Eisenberg, *J. Am. Chem. Soc.*, 1996, **118**, 3168-3181.

22. K. Yu and A. Eisenberg, *Macromolecules*, 1996, **29**, 6359-6361.
23. Z. F. Jia, X. W. Xu, Q. Fu and J. L. Huang, *J. Polym. Sc., Part A: Polym. Chem.*, 2006, **44**, 6071-6082.
24. P. Lim Soo and A. Eisenberg, *J. Polym. Sci. Part B: Polym. Phys.*, 2004, **42**, 923-938.
25. T. Qu, A. Wang, J. Yuan, J. Shi and Q. Gao, *Coll. Surf. B: Biointerfaces*, 2009, **72**, 94-100.
26. M. L. Adams, A. Lavasanifar and G. S. Kwon, *J. Pharm. Sci.*, 2003, **92**, 1343-1355.
27. Y. Li, B. S. Lokitz, S. P. Armes and C. L. McCormick, *Macromolecules*, 2006, **39**, 2726-2728.
28. W. Zauner, N. A. Farrow and A. M. R. Haines, *J. Controlled Release*, 2001, **71**, 39-51.
29. J. Zastre, J. Jackson, M. Bajwa, R. Liggins, F. Iqbal and H. Burt, *Eur. J. Pharm. Biopharm.*, 2002, **54**, 299-309.
30. J. Panyam and V. Labhasetwar, *Pharm. Res.*, 2003, **20**, 212-220.
31. Y. Kim, M. H. Pourgholami, D. L. Morris and M. H. Stenzel, *Macromol. Bioscience*, 2011, **11**, 219-233.
32. G. Moad, E. Rizzardo and S. H. Thang, *Aust. J. Chem.*, 2012, **65**, 985-1076.
33. E. Rizzardo and D. H. Solomon, *Aust. J. Chem.*, 2012, **65**, 945-969.
34. X. Huang, X. Jiang, Q. Yang, Y. Chu, G. Zhang, B. Yang and R. Zhuo, *J. Mater. Chem. B*, 2013, **1**, 1860-1868.
35. Y. Zhao, M. S. Lord and M. H. Stenzel, *J. Mater. Chem. B*, 2013, **1**, 1635-1643.
36. J. Li, W. Zhang, Z. Hu, X.-J. Jiang, T. Ngai, P.-C. Lo, W. Zhang and G. Chen, *Polym. Chem.*, 2013, **4**, 782-788.
37. F. Yhaya, S. Binauld, M. Callari and M. H. Stenzel, *Aust. J. Chem.*, 2012, **65**, 1095-1103.
38. M. A. Harvison, P. J. Roth, T. P. Davis and A. B. Lowe, *Aust. J. Chem.*, 2011, **64**, 992-1006.
39. M. H. Stenzel, *Chem. Commun.*, 2008, 3486-3503.
40. S. E. Burke and A. Eisenberg, *Langmuir*, 2001, **17**, 6705-6714.
41. Q. Ma, E. E. Remsen, C. G. Clark, T. Kowalewski and K. L. Wooley, *PNAS*, 2002, **99**, 5058-5063.
42. L. Zhang and A. Eisenberg, *J Am Chem Soc*, 1996, **118**, 3168-3181.
43. H. T. T. Duong, T. L. U. Nguyen, J. Kumpfmüller and M. H. Stenzel, *Aust. J. Chem.*, 2010, **63**, 1210-1218.
44. A. Lavasanifar, J. Samuel and G. S. Kwon, *Advanced Drug Delivery Reviews*, 2002, **54**, 169-190.
45. Y. Kim, E. D. Liemmawal, M. H. Pourgholami, D. L. Morris and M. H. Stenzel, *Macromolecules*, 2012, **45**, 5451-5462.
46. Y. Kim, M. H. Pourgholami, D. L. Morris and M. H. Stenzel, *Biomacromolecules*, 2012, **13**, 814-825.
47. Y. Kim, M. H. Pourgholami, D. L. Morris, H. Lu and M. H. Stenzel, *Biomater. Sci.*, 2013, **1**, 265-275.